

COMPUTATION OF THE LONGITUDINAL SPACE CHARGE EFFECT IN PHOTOINJECTORS *

C.Limborg-Deprey*, P.Emma, Z.Huang, J.Wu

SLAC, MS 18 , Menlo Park CA 94025, USA

Abstract

The LCLS Photoinjector produces a 100A, 10 ps long electron bunch which is later compressed down to 230 fs to produce the peak current required for generating SASE radiation. SASE saturation will be reached in the LCLS only if the emittance and uncorrelated energy spread remain respectively below 1.2 mm.mrad and 5.10^{-4} . This high beam quality will not be met if the Longitudinal Space Charge (LSC) instability develops in the injector and gets amplified in the compressors. The LSC instability originates in the injector beamline, from an initial modulation on top of the photoelectron pulse leaving the cathode. Numerical computations, performed with Multiparticle Space Charge tracking codes, showing the evolution of the longitudinal phase space along the LCLS injector beamline, are discussed. Their results are compared with those deduced from theoretical models in different regimes of energy and acceleration and for different modulation wavelengths. This study justifies the necessity to insert a "laser heater" in the LCLS Photoinjector beamline.

LONGITUDINAL SPACE CHARGE

Description

A current density modulation transforms into energy modulation due to longitudinal space charge forces. An energy modulation transforms into current modulation at low energy due to the large relative spread of velocities. For low energy charged beam, these periodic oscillations are well known as "plasma oscillations".

In the photoinjector, the irregularities on top of the laser profile transfer into the electron beam current profile during photoemission. These modulations create microstructures in the longitudinal phase space, which can prevent operation of the FEL. Indeed, the bunching factor gets amplified in the bunch compressors. It transfers into slice energy spread and increases the saturation length, preventing the beam undergoing SASE to reach saturation, or even lasing.

A concern for the LCLS

Possible dangerous amplification of the bunching due to the LSC has first been expressed for TTF2 [1]. Strong micro-bunching due to longitudinal space charge forces has been observed and experimentally characterized at the DUVFEL [2].

For the TTF2 parameters, it was demonstrated that the LSC instability should be damped at the early stage of acceleration. For the LCLS parameters, simulations show that small modulations of current density (a few %) could

prevent operation of the SASE FEL. However, the micro-bunching induced by the LSC will not get amplified if sufficient uncorrelated energy spread is introduced soon early in the accelerating process. The LCLS Superconducting wiggler located at the end of Linac1 had to be traded for a "Laser Heater" to be installed at the end of Linac0. The "Laser Heater" increases the uncorrelated energy spread from 3keV to 40keV. This is enough to prevent both developments of the LSC instability and of the micro-bunching instability due to CSR[3].

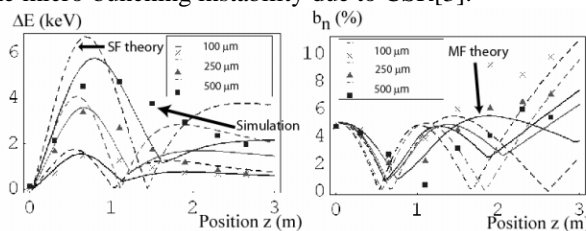


Figure 1- Energy modulation and Current modulation for a 6MeV beam along a drift; comparison with theory for single (SF) and multiple frequency (MF)

LSC IN DRIFTS

Comparisons between simulations and theory were done in the case of ~3 m long drifts for 3 different energies 6, 12 and 120MeV using PARMELA [4] and ASTRA[5].

PARMELA Simulations

The beam had dimensions close to those of the LCLS beam at a position $z = 70$ cm downstream of the cathode, but it was monoenergetic. 40k particles and 400 meshes along the bunch were used. For the lower energy cases, 6MeV and 12 MeV, the initial beam was transversally converging with an rms beam size varying from 1mm down to 0.5 mm and up to 3.7 mm. The modulations with period 100, 250 and 500 μ m on top of the hypergaussian current profile had a relative amplitude of 5%.

After removal of the RF-induced correlations, the oscillation of the energy centroid along the bunch is recorded. A narrow-band filtering is performed on the Fourier transform of the current profile. The high frequency noise introduced by the meshing is thus removed. The amplitude of the modulation is then quantified after an inverse Fourier transform has been done. Evolution of energy and current modulations are summarized in figures 1.

ASTRA Simulations

For the ASTRA simulations, the bunch length was chosen to be of 24 wavelengths. Data were analyzed for the core 36% of the bunch to minimize edge effects from head and

tails. The number of mesh points was chosen to be of ~ 12 per wavelength and 1 million particles were used. A systematic study of linearity and number of mesh points was done for the 120MeV case for the very short wavelengths 15 and 30 μm . Results demonstrated a good linearity between 1% and 5% initial amplitude of modulation. It also proved that the use of more than 5 mesh points per wavelength, generates too large numerical noise from the scheff routine.

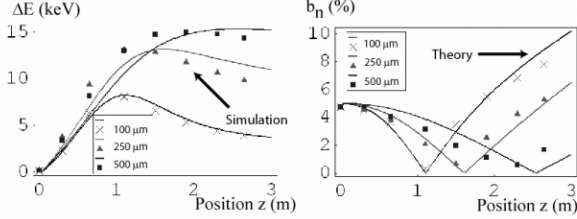


Figure 2- a-b Energy modulation / Current modulation for a 12 MeV beam along a drift; comparison with theory for single and multiple frequency

Theory

The LSC impedance per unit length in free space is:

$$Z(k) = \frac{iZ_0}{\pi k r_b^2} \left[1 - \frac{kr_b}{\gamma} K_1 \left(\frac{kr_b}{\gamma} \right) \right], \quad (1)$$

where $Z_0 = 377 \Omega$, r_b is the beam radius for a uniform transverse distribution, K_1 is the modified Bessel function. A weak transverse dependence of the LSC field is neglected here.

The current modulation (characterized by the bunching spectrum $b(k)$) for a coasting beam at the position s in a linac is given by the integral equation

$$b(k, s) = b(k, 0) + ik \frac{I}{I_A} \int_0^s d\tau R_{56}'(\tau \rightarrow s) \frac{4\pi Z(k, \tau)}{Z_0} b(k, \tau), \quad (2)$$

where I is the beam current, $I_A \approx 17$ kA is the Alfvén current, and the generalized momentum compaction factor R_{56}' is the ratio of the path length change at s due to a small change in γ at τ , given by

$$R_{56}'(\tau \rightarrow s) \approx \int_{\tau}^s \frac{ds'}{\gamma(s')^3}, \quad \text{for } \gamma \gg 1 \quad (3)$$

Equation (2) generalizes the integral equation for CSR microbunching in a bunch compressor [6,7] to an linac with acceleration, and ignores any Landau damping in the linac. For example, in a simple drift space, $R_{56}' = (s - \tau)/\gamma^3 = R_{56}/\gamma$ and Eq. (2) produces the well-known solution of the space charge oscillation. If the beam size and electron energy vary along the linac, Eq. (2) can be solved numerically to obtain the evolution of the current modulation.

The change in energy modulation in the linac is then

$$\Delta\gamma(k, s) = \Delta\gamma(k, 0) - \frac{I}{I_A} \int_0^s d\tau Z(k, \tau) b(k, \tau). \quad (4)$$

At sufficiently high energy or large γ , we have $R_{56}' = 0$ and the beam current modulation is frozen [1], i.e., $b(k, s)$

$= b_0(k)$. Thus, the energy modulation is accumulated according to

$$\Delta\gamma(k, s) = \Delta\gamma(k, 0) - \frac{I b(k, 0)}{I_A} \int_0^s d\tau \frac{4\pi Z(k, \tau)}{Z_0}.$$

Comparison with theory

The variation of charge density due to transverse dimensions had to be taken into account [6] in the theoretical model. A model which included the radial dependency of the space charge impedance could not explain the remaining discrepancy between simulations and theory.

The agreement is quite good for both the energy modulation and the bunching for the 12 MeV and 120 MeV cases (see figure 2). For the 6MeV case, the theory does not agree as well with the results from the simulations. The theory shows that the energy modulation amplitude cancels. This was never observed in any of the simulation cases studied. As the beam is travelling along the drift, the frequency spectrum of the energy modulation is no longer a single line, but has a much broader extension. Computed with multiple frequencies, the theoretical curve of the energy modulation does not go back to zero and gets closer to the simulation curve in the bunched beam case of the PARMELA simulations. The exact current density was not taken into account in figure 1 but should only give a few percent correction. The spread in frequencies has been computed for a gaussian bunch and not for an hypergaussian one. The theoretical model does not include either the growth in uncorrelated energy spread, which is clearly visible in simulations. It is still unclear how much this increase in uncorrelated energy spread, shown by the simulations, is due to numerical noise or if it has some physical reality. Those aspects might explain the remaining discrepancy between theory and simulations.

Comparison theory and simulation

A 6MeV beam with the typical LCLS transverse parameters, but starting monoenergetic, travels through a 90 cm drift and is then accelerated up to 65 MeV in a 3m long accelerating section, and drifts 1 m before being accelerated up to 135 MeV. The agreement between the theory and the simulations is very good.

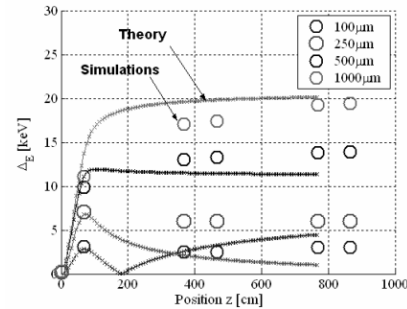


Figure 3- Simulations and theory for energy modulation for a drift + linac+ drift +linac system;

INJECTOR

Difficult simulations

Simulations of the longitudinal space charge instability for long wavelengths modulations, i.e. above 150 μm , do not present difficulties for the 3mm long LCLS bunch. Good sampling of the modulation period requires at least 5 mesh points per period. 150/600 longitudinal meshes are required to study 100 μm /25 μm modulations. With 15 radial mesh points and a minimum of 20 macro-particles per computation ring, more than 100k macro-particles are needed for the computation. With 100k macro-particles, the numerical noise is at the percent level, i.e. at the level of the amplitude of modulations studied. Those simulations require at least 1million particles. It is now possible to run 10 millions particles both with ASTRA and PARMELA in a humanly affordable time on the 2004 generation of PCs.

To study short wavelength modulation, a new option has been provided in ASTRA to increase locally the number of macro-particles and to allow irregular meshing. Macro-particles charges are weighted in order to represent the correct current density. The mesh is densified in that region.

Some Damping

Figures 4 a-b show the evolution of the energy modulation and of the current density modulation for initial laser modulations of 2.5 and 5%. There is strong damping of the current density modulation in the gun and in the drift to the entrance to L01. Very small energy modulation is generated in the gun, but it becomes large in the drift to the entrance of the L01. One will notice the evolution in quadrature between energy and current density at the entrance of L01. Amplitudes both of energy and current do not scale linearly with the initial modulation on the laser and saturation seems to occur in the gun. A theoretical description of this saturation mechanism still needs to be given. Simulations with higher numbers of particles (~10 millions) will be run to confirm the numbers. Those results, obtained with ASTRA, are in qualitative agreement with those obtained with PARMELA for higher amplitude of modulation. However, both simulations show that in the gun the growth of the instability is not linear with the initial amplitude of modulation. At higher energies, the linearity was checked to be perfect at least up to 5% amplitude of modulation.

CONCLUSION

A good agreement has been obtained between simulations and theory of the LSC instability for energies higher than 10MeV. Some aspects of the theory are still missing for the very low energies. Multiple frequency modulations remain to be studied as the dynamics are here very non-linear. The LCLS laser bandwidth, with 3 nm (equivalent to 11.1THz), will be large enough so that the initial modulation of the Fourier limited pulse will not exceed

the 1% level even for the 0.7 ps rise/fall times. Also, its modulation wavelength will be smaller than 25 μm . Other sources of modulation might still need to be identified and controlled. The 40 keV uncorrelated energy spread added with the "Laser Heater" to the beam will be sufficient to prevent the amplification of the microbunching in the linac.

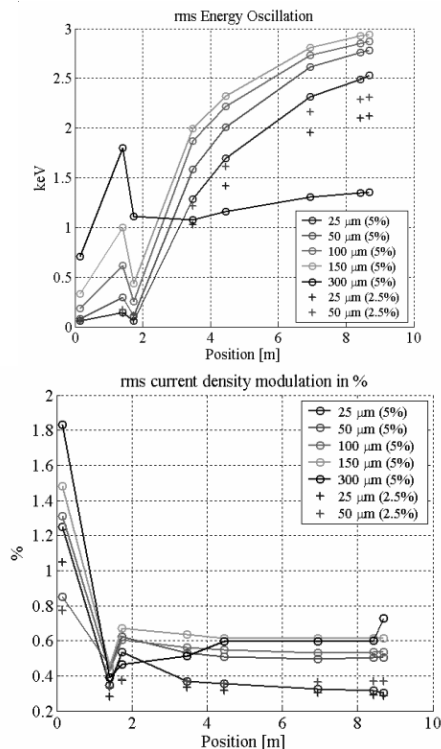


Figure 4-a-b- rms energy oscillation and current density modulation along the LCLS photoinjector beamline.

Acknowledgements

The authors wish to thank T.Shaftan, M.Borland, G.Stupakov, Y.Kim and K.Floettmann for very valuable discussions. Particular thanks go to K.Floettmann for introducing the merge option in ASTRA.

REFERENCES

- [1] E.L.Saldin et al. "Longitudinal Space Charge Driven microbunching instability at TTF2", TESLA-FEL-2003-02
- [2] T.Shaftan et al. "Microbunching and Beam Break-up in DUV FEL Accelerator", PAC 03,
- [3] Z.Huang et al. , contribution WEPLT156 to these proceedings
- [4] ASTRA, K.Floettmann <https://www.desy.de/~mpyflo/>
- [5] L.Young, J.Billen , PARMELA, LANL Codes, laacg1.lanl.gov/laacg/services/parmela.html
- [6] S. Heifets, G. Stupakov, and S. Krinsky, Phys. Rev. ST Accel. Beams **5**, 064401 (2002).
- [7] Z. Huang and K.-J. Kim, Phys. Rev. ST Accel. Beams **5**, 074401 (2002).